Proc. Indian Acad. Sci. (Chem. Sci.), Vol. 92, Numbers 4 & 5, August & October 1983, pp. 527–542.

XANES and EXAFS of copper compounds: Studies of copper carboxylates with metal-metal bonds and of the complex formed by *Pseudomonas aeruginosa*†

P R SARODE, G SANKAR and C N R RAO*

Solid State and Structural Chemistry Unit, Indian Institute of Science, Bangalore 560012, India.

Abstract. X-ray absorpion near edge structure (XANES) of copper compounds with copper in 1^+, 2^+ and 3^+ states has been studied. Extended x-ray absorption fine structure (EXAFS) has been employed to determine bond distances and coordination numbers in several model copper compounds. Employing both XANES and EXAFS, the structure of the copper complex formed by the micro-organism *Pseudomonas aeruginosa* has been shown to be square-planar with the Cu–O distance close to that in cupric glucuronates and cupric acetylacetonate. EXAFS has been shown to be useful for studying metal-metal bonds in copper carboxylates.

Keywords. XANES; EXAFS; copper compounds; x-ray spectra.

1. Introduction

X-ray absorption near edge structure (XANES) and extended x-ray absorption fine structure (EXAFS) have become powerful tools for studies in elucidating the structure of various compounds (Belli *et al* 1980; Parthasarathy *et al* 1982; Sankar *et al* 1983). XANES provides information about the nature of coordination in metal compounds, while EXAFS gives bond distances besides the coordination numbers. These tools are especially useful for investigating biological compounds, amorphous materials and other systems which may not be available in the form of single crystals for crystallographic studies. In this paper we describe the results of our investigation of copper compounds employing both XANES and EXAFS. After having verified the results from these techniques with respect to model compounds, we have used the techniques to elucidate the structure of copper complex formed from the slime of the *Pseudomonas aeruginosa*. This micro-organism accumulates copper to a considerable extent and little is known about the actual structure of the copper complex so formed (Payne *et al* 1981). We have also examined the use of EXAFS to study copper carboxylates containing metal-metal bonds. These studies have been able to establish square-planar coordination in the copper complex formed from *Pseudomonas aeruginosa* and also provides the metal-oxygen bond distances in the complex as well as in model copper glucuronates.

2. Experimental

Analar samples of $CuSO_4 \cdot 5H_2O$ and $CuCl_2 \cdot 2H_2O$ were obtained commercially. All other copper (I) and (II) compounds were prepared by standard methods (Brauer 1963).

† Communication No. 228 from the Solid State and Structural Chemistry Unit

* To whom all correspondence should be addressed.

$Ba_2Cu_2O_5$ was prepared by the method of Arjomand and Machin (1975). Cupric glucuronates and copper complex formed from *Pseudomonas aeruginosa* were prepared by the methods already reported (Payne *et al* 1981).

X-ray absorption spectra were recorded using a bent-crystal spectrograph. The absorbers of the compounds were prepared by spreading the finely-powdered specimen on cellophane adhesive tape. The energy scale was fixed by using the emission lines of tungsten which appeared due to the impurity in the target. A Carl-Zeiss MD 100 densitometer was used to obtain the traces of these photographically recorded spectra. In order to obtain finer details of the spectra, 200 × magnification scans were taken for each compound. The linear reverse dispersion on the traces in each case was 0·35 eV/mm. The uncertainty in the edge and its near structure at about 50 eV was ±0·5 eV and beyond 50 eV it was about 1 eV. We have been able to observe the fine structure beyond the edge upto about ~ 550 eV.

2.1 *Data reduction and analysis*

To extract the extended x-ray absorption fine structure modulation, $\chi(E)$ ($= (\mu - \mu_0)/\mu_0$, where μ is the observed absorption coefficient and μ_0 is the absorption coefficient modulation in the absence of neighbouring atoms) from the raw absorption spectra, background subtraction was done using a method due to Lytle *et al* (1975). This involves the fitting of a polynomial (Victoreen function) to the pre-edge portion of the raw data and extrapolating it over the whole range of the absorption data and subtracting it. After this pre-edge subtraction, a second degree polynomial is fitted through the centre of EXAFS oscillations. This curve is assumed to be the μ_0 *vs* energy curve and subtracted from the data and the difference is then divided by it in order to get $(\mu - \mu_0)/\mu_0$. This procedure gives the normalized absorption coefficient as a function of photon energy. For structural analysis, the normalized fine structure was obtained as a function of photoelectron wavevector, k, (in Å^{-1}), defined by the relation $k = [0{\cdot}262467\,(E - E_0)]^{1/2}$ eV, where E is the photon energy and E_0 the threshold energy at the absorption edge. The data thus obtained was multiplied by the Hanning window function (Via *et al* 1979) in order to minimize the termination ripples. Subsequently, it was multiplied by a weighting function, k^3, to compensate for amplitude reduction as a function of k. The integrations (integration limits $k = 3{\cdot}5$ to $k = 11{\cdot}6\ \text{Å}^{-1}$) for the Fourier transforms, both for the real and imaginary components, were done numerically using Simpson's rule (Cramer *et al* 1978). The modulus of the Fourier transform was obtained as a square root of the sum of the real and imaginary parts.

The extended x-ray absorption fine structure associated with the K-absorption edge was shown to have (in terms of structural parameters) the following general form (Stern 1974; Ashley and Doniach 1975):

$$\chi(k) = \frac{\mu - \mu_0}{\mu_0} = \frac{1}{k}\sum_j \frac{N_j}{R_j^2} |f_j(\pi, k)| \exp(-\sigma_j^2 k^2) \exp(-2R_j/\lambda) \sin[2kR_j + \phi_j(k)]. \quad (1)$$

In this expression, N_j is the number of scatterers (j) at distance R_j from the absorber; $f_j(\pi, k)$ is the scatterer's electron backscattering amplitude; ϕ_j is the total phase shift; σ_j^2 is the mean square deviation of R_j, λ is the mean free path and k is the photoelectron wave vector. A separate modulation or wave in the absorption coefficient is produced by each coordination shell of atoms of approximately the same distance R_j from the

absorbing atom. The observed fine structure results from the sum of waves from the various coordination shells. The object of the data analysis procedure is to decompose the observed spectrum into its component waves and determine the phase and amplitude of each component. This in turn can yield information about the distance in the coordination shells and the number of atoms in them.

A least-squares curve fitting analysis was employed to elucidate finer details of the structure of compounds. The background subtracted absorption data were first Fourier-transformed and then the region of interest in FT plot was Fourier-filtered to isolate the first and second coordination shells. Six parameter fits were performed on the data using a parametrized form of equation (1)

$$\chi_{\text{param}} = C_0 \cdot \exp(C_1 k^2)/k^{C_2} \sin(a_0 + a_1 k + a_2/k). \tag{2}$$

Fits were done by least-squares adjustment of parameters C_0, C_1, C_2, a_0, a_1 and a_2 using a general optimization technique (Himmelblau 1972). The function minimized in the fitting procedure is given by

$$F = \left[\frac{\sum k^6(\chi_{\text{expt}} - \chi_{\text{param}})^2}{N}\right]^{1/2}, \tag{3}$$

where χ_{param} is the parametrized EXAFS function, χ_{expt} is Fourier filtered EXAFS function, N is the number of data points in the fit and the sum is over the number of data points. F is a measure of the goodness of the fit and is lower for a better fit.

The curve fitting procedure for determining the distance R to a shell of atoms in an unknown compound is as follows. EXAFS data from a model compound whose crystal structure is known is fitted with equation (2) by adjusting all the six parameters. The standard parameters C_1, C_2, a_0 and a_2 are then used as fixed constants in fitting (2) to data from the unknown compound by adjusting only C_0 and a_1. If the phase shift $\phi(k)$ is assumed to have the form $\phi(k) = a_0 + a_1 k + a_2/k$, then comparison of the theoretical equation (1) with the parametrized equation (2) shows that $a_1 = 2R + \phi$. The linear phase parameter ϕ is determined from the standard fit since R is known, and then ϕ is used to calculate R from the fit of the unknown. After determining R_2 for the unknown, the number of atoms N can be estimated by $N = (C_0/C_{os})(R_s/R)$ where N, R and C_0 refer to the unknown and N_s, R_s and C_{os} refer to the model compound.

3. Results and discussion

3.1 *XANES of typical copper compounds*

Figures 1 and 2 show plots of K-absorption edges of representative of copper compounds with copper in 1^+, 2^+ and 3^+ states; the figure also includes absorption edges of a few copper complexes. In the case of Cu^{2+} compounds (figure 1) we are able to make spectral assignments on the basis of the assignments available for other transition metal compounds (Sankar *et al* 1983; Shulman *et al* 1976). The small pre-edge peak at about 8977·5 eV is due to the vibronically activated $1s \rightarrow 3d$ transition. The next feature in the spectra appearing as a shoulder is attributed to the forbidden $1s \rightarrow 4s$ transition, which appears to become allowed due to the mixing of the $4p$ and $4s$ orbitals. The highest energy peaks in the spectra arise from the allowed $1s \rightarrow 4p$ transition which ultimately merges into the continuum. The consistency in the position of the peaks due to the $1s \rightarrow 3d$ transition is noteworthy; the energies of $1s \rightarrow 4s$ and $1s \rightarrow 4p$ transitions

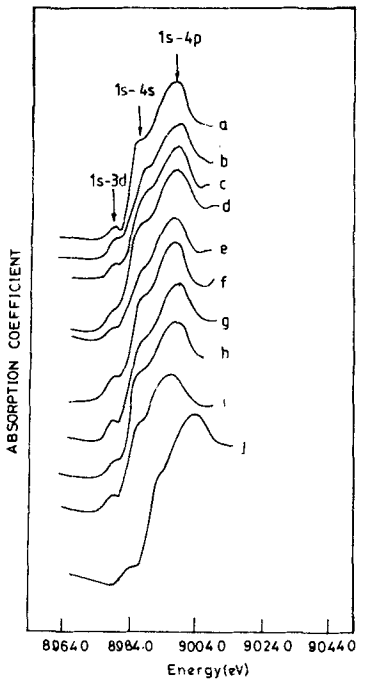

Figure 1. Copper *K*-edge absorption spectra of (a) cupric oxide; (b) copper propionate; (c) copper citrate; (d) sodium copper glucuronate; (e) barium copper glucuronate; (f) magnesium copper glucuronate; (g) copper complex from *Pseudomonas aeruginosa*; (h) cesium copper trichloride; (i) cupric chloride dihydrate; (j) $Ba_2Cu_2O_5$.

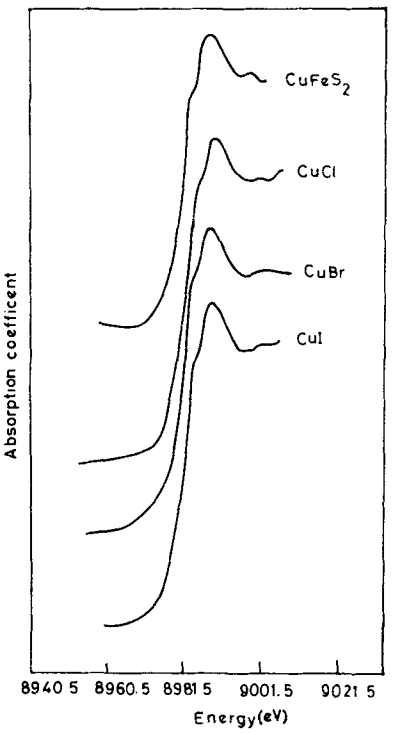

Figure 2. Copper *K*-edge absorption spectra of $CuFeS_2$; CuCl, CuBr and CuI.

show a similar behaviour. Energies of these three electronic transitions for several Cu^{2+} compounds are listed in table 1. The energy range for the $1s \rightarrow 3d$ transition is 8977·3–8978·3 eV with an average of 8977·8 eV. The standard deviation of this average for the Cu^{2+} compounds studied is only 0·6 eV. The energy range for the $1s \rightarrow 4s$ transition is 8985–8987 eV with an average 8986 eV and a standard deviation of 0·8 eV. The average energy for $1s \rightarrow 4p$ is 8996·5 eV.

Absorption edges of a few Cu^{1+} compounds are shown in figure 2. The first peak which appears as a shoulder, in the spectrum of the Cu^{1+} compounds is due to the $1s \rightarrow 4s$ transition, the $1s \rightarrow 3d$ transition being absent in this d^{10} system. The $1s \rightarrow 4s$ transition of Cu^{1+} comes at a lower energy than Cu^{2+}. The energy of the $1s \rightarrow 4s$ transition of Cu^{1+} is 8982·6 eV and this does not overlap with either the $1s \rightarrow 3d$ or $1s \rightarrow 4s$ range found in Cu^{2+} compounds, thus providing a clear distinction between the edge spectra of the compounds with copper in the two different oxidation states. As mentioned earlier, it is noteworthy that there is no $1s \rightarrow 3d$ transition in Cu^{1+} compounds and this again enables the distinction between Cu^{1+} and Cu^{2+} spectra.

Table 1. X-ray K-absorption edge data on copper compounds.

Compound	Transition energies (eV)		
	$1s \rightarrow 3d$	$1s \rightarrow 4s$	$1s \rightarrow 4p$
Copper ammonium sulphate monohydrate	8978·0	8984·3	8994·0
Cupric oxide	8978·2	8985·0	8995·6
Anhydrous copper propionate	8977·8	8985·7	8995·9
Copper sulphate pentahydrate	8977·4	8986·5	8996·6
Copper citrate dihydrate	8977·9	8985·8	8996·0
Cesium copper trichloride	8977·3	8985·9	8997·5
Cupric chloride dihydrate	8977·6	8987·0	8996·0
Sodium copper glucuronate	8977·5	8985·1	8995·3
Barium copper glucuronate	8977·4	8985·0	8995·4
Magnesium copper glucuronate	8977·4	8985·1	8995·1
Copper complex formed from *Pseudomonas aeruginosa*	8978·3	8985·3	8995·5

Differences in the spectra of compounds with copper in the 2^+ and 3^+ states are small compared to the differences between the spectra of Cu^{1+} and Cu^{2+} compounds. $Ba_2Cu_2O_5$ containing copper in the Cu^{3+} state shows a pre-edge transition (figure 1) with a peak at 8985 eV, about 8 eV above the highest energy found in Cu^{2+} compounds. The peak position of the $1s \rightarrow 4s$ transition is found at 8995 eV, 10 eV higher than that of Cu^{2+} compounds.

3.2 *EXAFS of typical copper compounds*

In figure 3 we show background subtracted spectra of cupric oxide, anhydrous copper propionate, copper ammonium sulphate monohydrate and copper thiosalicylate. In figure 4 we have shown the Fourier-transformed spectra in R-space of these compounds. These are the four-model compounds used to identify near neighbours by determining the phase shift for Cu–O, Cu–Cu, Cu–N and Cu–S atom pairs. Except for the copper propionate, each of these has a major peak in the FT plot (single-shell model compounds)*. This intense peak is isolated using a suitable window function (Teo 1981) by retransforming it to k-space and then fitted with (2) by adjusting all six parameters C_0, C_1, C_2, a_0, a_1 and a_2. The first two peaks in the copper propionate transform were retransformed to k-space and fitted with the sum of two waves in two-shell fit. The first shell contains the amplitude and phase parameters from the cupric oxide fit, adjusting only C_0 and a_1, while all the six parameters of the second shell corresponding to Cu–Cu atom pair were adjusted. Table 2 lists the results of the fits of these model compounds including the fitting function value from (3), and the parameters C_0, C_1, C_2, a_0, a_1, and a_2 from (2). In figure 5, we have shown the fitted and experimentally observed (Fourier-filtered) EXAFS spectra of these model compounds. The curve-fitted spectra obtained from the parameterized form of EXAFS equation matches very well with the observed Fourier-filtered spectra. According to Citrin *et al* (1976) and Cramer *et al* (1978) all these phase (a_0, a_1, a_2) and amplitude (C_0, C_1, C_2) parameters can be transferred to the

* The term single shell refers to structures where the absorbing atom is surrounded by a set of identical scatterers at nearly equal distances.

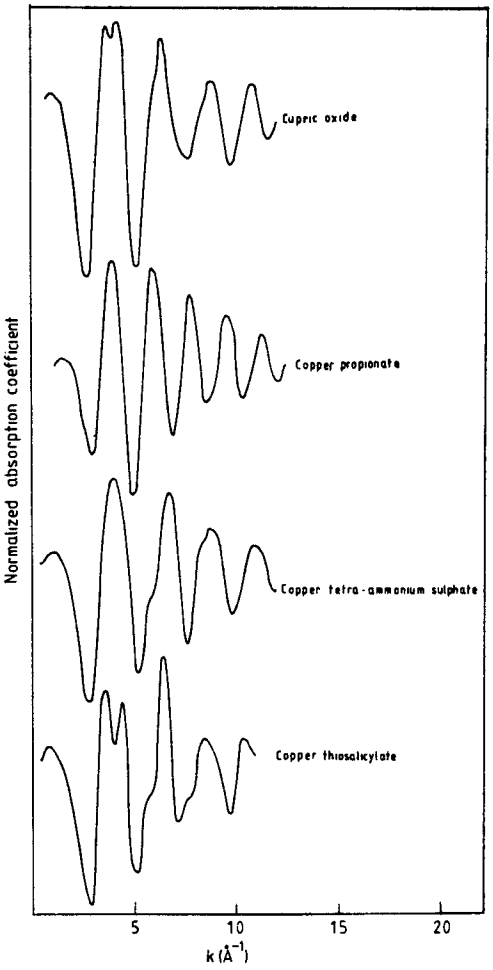

Figure 3. Background-subtracted EXAFS spectra of four model compounds.

system in which the absorbing atoms have the same environments to predict the structural parameters. As a first test of transferability of these Cu-X parameters, these phase shifts and amplitudes were used to determine other crystallographically known compounds. The compounds chosen for this test were copper sulphate pentahydrate, copper acetylacetonate and copper phthalocyanine all of which possess square-planar co-ordination (Bacon and Curry 1962; Basu *et al* 1962; Harrison and Assour 1964) and bond distances comparable to those in CuO. The Fourier-transformed spectra for these compounds are shown in figure 6. To obtain structural information from the FT spectra of these compounds, the observed peak position is simply modified by previously determined phase shift to obtain a predicted distance. The co-ordination number is then obtained from the observed peak height. The predicted and crystallographically observed structural results are summarized in table 3.

For curve-fitting analysis of the spectra, C_0, and a_1 were floated while C_1, C_2, a_0 and

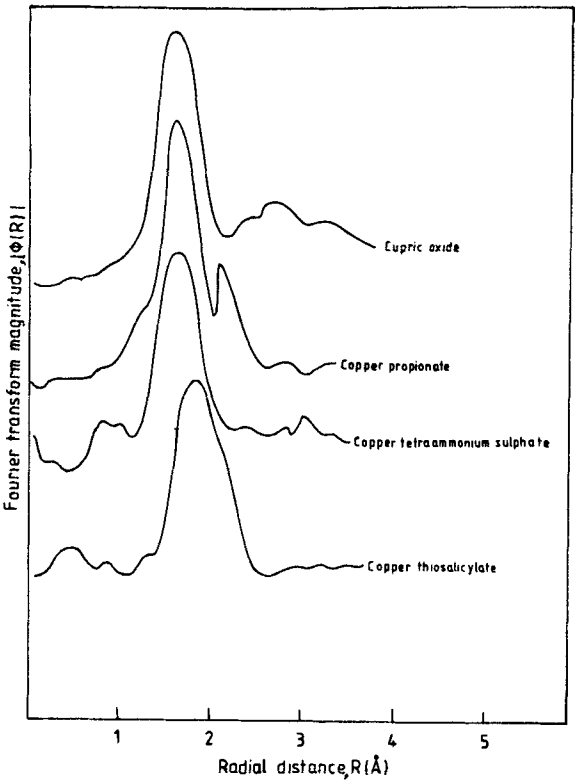

Figure 4. Fourier transforms of the four model copper compounds. Curves shows the magnitude only. Transform range: 3·5–11·6 $Å^{-1}$, k^3 scaling.

a_2 were fixed. The two parameters floated gave bond lengths and co-ordination numbers. The numerical results of these fits are presented in table 3. We see that the predicted bond distances and co-ordination numbers from EXAFS agree with those obtained from x-ray diffraction data. The close correspondence between the distances and the co-ordination numbers given by crystallography and EXAFS of the same compounds lends confidence to our ability to predict co-ordinating atoms and distances in copper compounds of unknown structure.

3.3 *XANES and EXAFS studies of copper glucuronates and the copper complex formed by the slime of Pseudomonas aeruginosa*

Edge spectra for sodium-copper glucuronate, barium copper glucuronate, magnesium copper glucuronate and a copper complex isolated from the slime of the *Pseudomonas aeruginosa* bacteria are shown in figure 1. These spectra show a weak peak in the Cu^{2+} $1s \rightarrow 3d$ region. The average energy of the $1s \rightarrow 3d$ peak in these complexes in 8977·6 eV. The next feature due to $1s \rightarrow 4s$ transition appearing as a shoulder is at 8985·1 eV. Both these transition energies are well within the range of Cu^{2+} compounds (see table 1). We can therefore conclude that copper in all these four copper complexes are in Cu^{2+} state. Accordingly these complexes show characteristic ESR signals due to Cu^{2+} (Payne *et al*

Table 2. Curve-fitting phase and amplitude parameters for a k range of 3·5–11·6 A^{-1}. (Optimized function, $\chi_{param} = [C_0.\exp(-C_1k^2/k^{C_2})] \cdot \sin(a_0 + a_1k + a_2/k$; k^6 weighting).

Standard atom pair[a]	Value of the fitting function[b]	C_0	C_1	C_2	a_0	a_1	a_2	Coordination number, N	Bond distance, R (Å)	Phase shift parameter, $\phi^{(g)}$ (Å)
Cu–N	0·89	0·824	−0·0146	1·930	1·430	3·659	21·54	4	2·05[c]	−0·441
Cu–O	0·92	0·410	−0·0190	1·380	1·560	3·476	21·84	4	1·955[d]	−0·434
Cu–S	0·48	2·369	−0·0141	2·365	0·621	3·949	30·51	4	2·20[e]	−0·451
Cu–Cu	0·68	2·089	−0·0146	2·900	3·760	5·052	38·57	1	2·578[f]	−0·104

(*a*) Cu–N from copper ammonium sulphate, Cu–O from cupric oxide, Cu–S from copper thiosalicylate and Cu–Cu from copper propionate; (*b*) From equation (3); (*c*) Mazzi (1955); (*d*) Asbrink and Norrby (1970); (*e*) Srivastava and Nigam (1972); (*f*) Simonov and Malinovskii (1970); (*g*) Calculated from $\phi = a_1 - 2R$

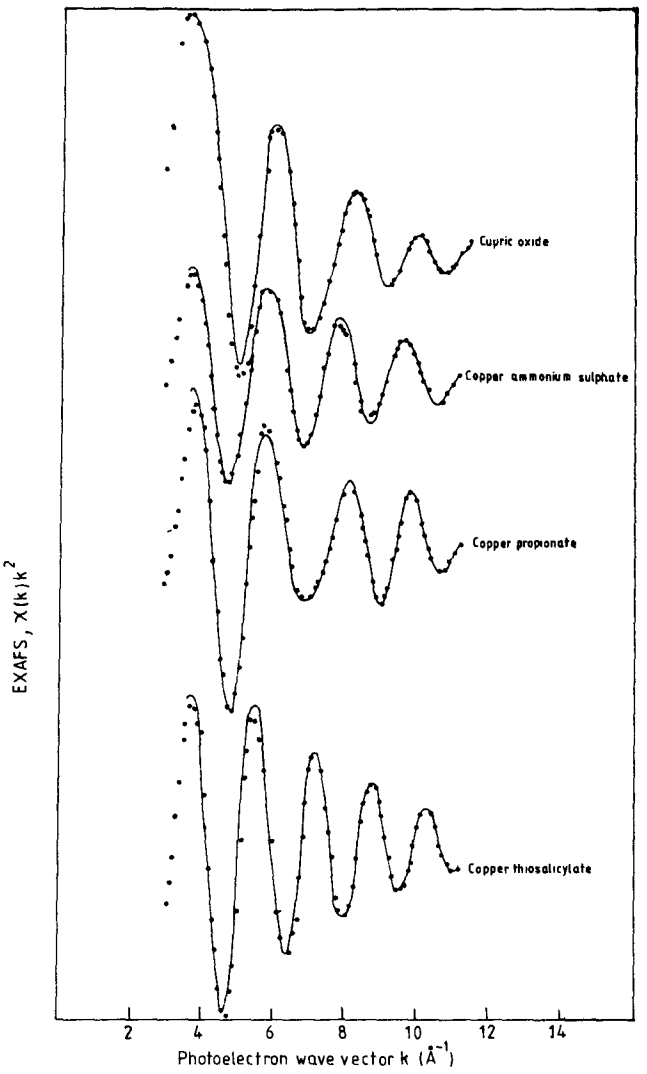

Figure 5. Fits of four model compounds. The solid lines are least-squares fits and the dotted lines are the Fourier filtered EXAFS data.

1981). Furthermore, the Cu($2p_{3/2}$) peaks in x-ray photoelectron spectra of these complexes exhibit characteristic satellites just as in CuO indicating the presence of Cu^{2+} ions (Payne *et al* 1981). It is well-known that near-edge structure gives information on the site symmetry of absorbing atoms in materials (Belli *et al* 1980; Grunes 1983). Since all the spectral features in the above complexes are essentially similar to those of Cu^{2+} model compounds where the coordination geometry of copper is square-planar, we may conclude that these cupric complexes are likely to have square-planar coordination. Thus, the ESR spectra of these copper complexes show $g_{\|}$ and $g_{\perp}$ values similar to cupric acetylacetonate (Payne *et al* 1981) confirming that the complexes are square-planar.

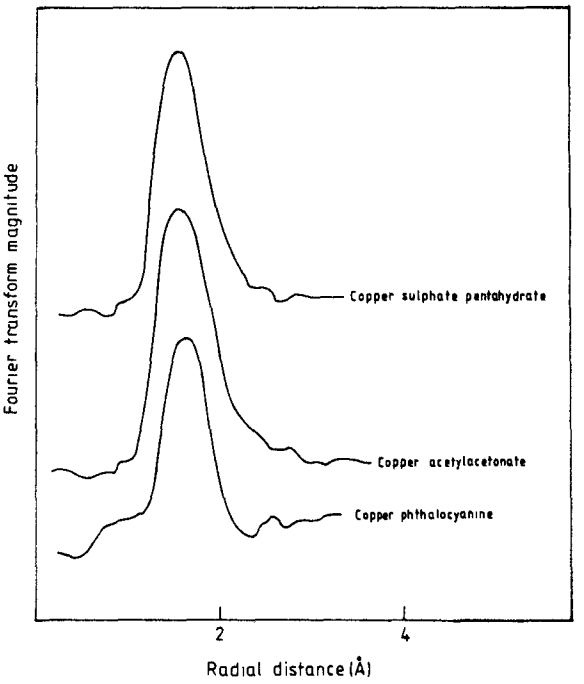

Figure 6. Fourier transforms of copper sulphate pentahydrate, copper acetylacetonate and copper phthalocyanine.

We shall now discuss the results of EXAFS analysis of these complexes. In (1), the total phase shift, ϕ, can be treated (Cramer and Hodgson 1979) as the sum of absorber, ϕ_a, and scatterer phase, ϕ_s shifts. $\phi(k) = \phi_a(k) + \phi_s(k)$. The absorber phase shifts $\phi_a(k)$ is the result of the photoelectron propagating out of and back through the central atom potential. Reflection of the photoelectron by the scattering atom potential causes the scatterer phase shift, ϕ_s. For a series of compounds with the same absorber, differences in total phase shift are caused by the different ϕ_s of the scattering atoms involved. The total phase shifts obtained from the experimentally measured EXAFS data as a function of wavevector are used to predict the type of atoms surrounding the absorbing atom.

In the present investigation, the total phase shifts were obtained by subtracting $2Rk$ from $a_0 + a_1k + a_2/k$ (for copper oxide, copper propionate, copper ammonium sulphate and copper thiosalicylate), k, ranging from 3·5 and 11·6 ($Å^{-1}$). In figure 7 we have plotted these empirical, pair-wise phase shifts for Cu–O, Cu–S, Cu–N and Cu–Cu; the curve for Cu–C pair could not be given since we do not have a model compound with carbon neighbour within 3Å range. In figure 8, we have plotted the phase shifts for the pairs taken from theoretically calculated and tabulated data of Teo and Lee (1979) and Lee *et al* (1977). Back scattering phase shifts for nitrogen are not given in the tables of these authors; the phase shifts for the Cu–N atom pair (figure 8) was obtained by interpolation as suggested by Teo and Lee (1979). We see from figures 7 and 8 that Cu–O, Cu–N, Cu–Cu and Cu–S phase shifts are all similar. The differences in phase shifts for O, Cu, N, S, permit straightforward differentiation between these back-scattering atoms. In figure 7, we have shown the dotted curve for the copper complex

Table 3. Calculation of single-shell distances and coordination numbers. Model compound: CuO.

Compound	Value of fitting function	C_0	a_1	Bond distance		Coordination number	
				FT distance (Å)	Curve-fit distance (Å)	FT number	Curve-fit number
Copper sulphate pentahydrate	0·62	0·421	3·506	2·00	1·97 (1·97)*	4·3+	4·2 (4·0)*
Copper acetylacetonate	0·79	0·399	3·446	1·96	1·94 (1·92)*	4·2+	4·1 (4·0)*
Copper phthalocyanine	0·92	0·813	3·239	1·85	1·84 (1·83)*	4·4+	4·2 (4·0)*
Sodium copper glucuronate	0·91	0·410	3·496	1·99	1·97	4·4+	4·1
Barium copper glucuronate	0·83	0·410	3·480	1·96	1·96	4·4+	4·2
Magnesium copper glucuronate	0·87	0·398	3·482	1·95	1·96	4·3+	4·1
Copper complex formed from *Pseudomonas aeruginosa*	0·94	0·396	3·487	1·99	1·96	4·3+	4·2

* Values in parenthesis are from x-ray diffraction data.

+ Coordination number determined from Fourier transform analysis, $N = R^2MN_s/M_sR_s^2$, where M_s, N_s and R_s are the observed peak height of the FT curve, coordination number and bond distance for a model compound respectively. Primed symbols refer to the unknown compound.

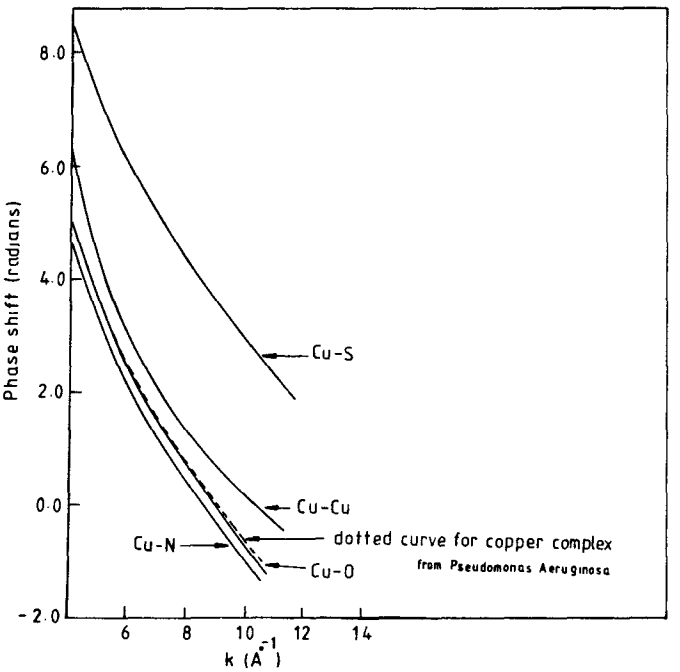

Figure 7. Experimentally determined copper-backscatterer phase shifts vs. photoelectron wave vector, k. 2π has been subtracted from the Cu–Cu phase shifts.

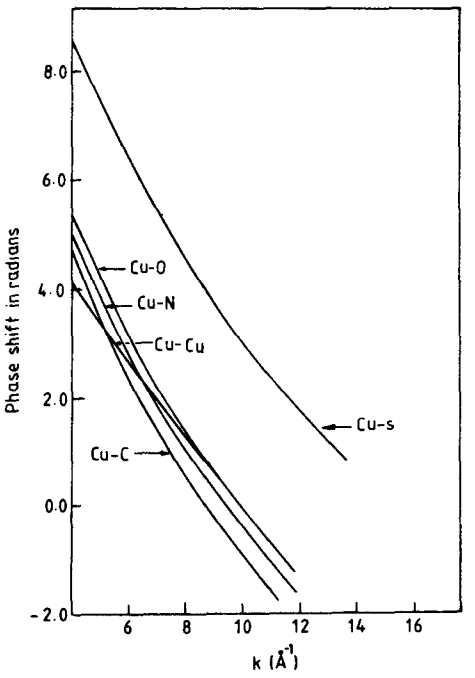

Figure 8. Theoretically calculated copper-backscatterer phase shifts vs. photoelectron wave vector, k. 2π has been subtracted from the Cu–Cu phase shifts.

formed from *Pseudomonas aeruginosa*. We see that the curve overlaps with that for the Cu–O atom pair once again establishing that copper in this complex has near neighbour oxygen atoms (in the first co-ordination shell); synthetic copper glucuronates also exhibit similar curves. After identifying the type of surrounding of copper in these complexes, we will now determine the bond distances and co-ordination numbers from EXAFS data.

In figure 9 we have shown the Fourier transform spectra of sodium copper glucuronate, barium copper glucuronate, magnesium copper glucuronate and complex obtained from *Pseudomonas aeruginosa*. The FT spectra retransformed to k-space and fitted to the parametrized equation (2) varying the amplitude parameter, C_0 and phase shift parameter a_1, while the other four parameters were fixed constant. The results of these analysis are summarized in table 3. As expected the co-ordination number in all these complexes is four establishing thereby that they are all square-planar. We readily see that the distances in the copper glucuronates and in the complex from *Pseudomonas aeruginosa* are quite similar to those of copper acetylacetonate.

Since the analysis of the slime produced by the bacteria *Pseudomonas aeruginosa* without copper present, using HPLC (Magee 1981) clearly shows that glucuronic acid is a major constituent, we suggest that the nature of the complex is itself copper glucuronate. The possible structures of the copper complex using the Haworth structure for the uronic acid is shown in chart I. In structure I, copper is co-ordinated

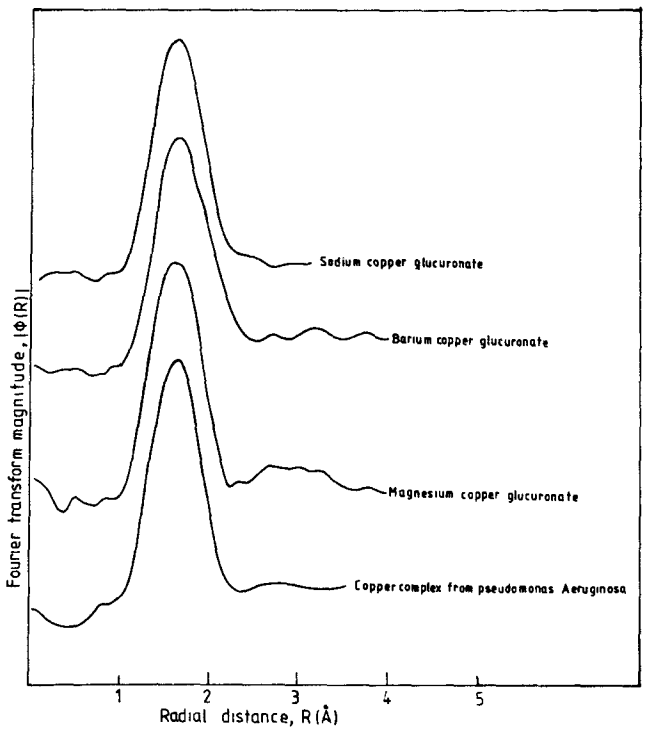

Figure 9. Fourier transforms of sodium copper glucuronate, barium copper glucuronate, magnesium copper glucuronate and copper complex formed from *Pseudomonas aeruginosa*.

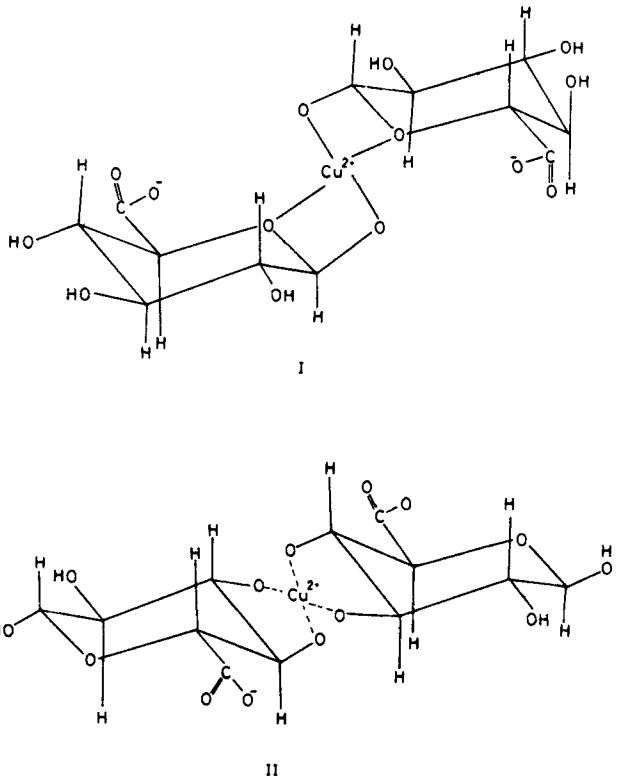

Chart 1.

through the ether oxygen of carbon 1 and the aldehydic oxygen. In structure II, copper is coordinated through the hydroxyl oxygens of carbon 3 and 4.

3.4 *Carboxylates with Cu–Cu bonding*

In order to determine whether a peak in the Fourier-transformed spectra corresponding to backscattering from a metal is sufficiently strong compared to those due to oxygen neighbours to be easily distinguished from them, EXAFS data were collected on few compounds with various metal-metal distances. Anhydrous copper propionate, copper acetate monohydrate, copper benzoate trihydrate, copper citrate dihydrate and copper salicylate tetrahydrate have Cu–Cu distances of 2·578 (Simonov and Malinovskii 1970), 2·614 (Brown and Chidambaram 1973), 3·15 (Inoue *et al* 1965), 3·242 (Mastropaolo *et al* 1976) and 3·728 Å (Inoue *et al* 1964) respectively. The Fourier-transformed spectra of these are shown in figure 10. In this figure the arrows show peaks corresponding to the Cu–Cu atom pairs. The propionate transform shows the Cu–Cu peak at 2·151 Å which means that the linear phase shift in R space for Cu–Cu pair is 0·427 Å. Applying this phase shift to the other transforms of the remaining three compounds, we have determined the Cu–Cu distances in these compounds. These distances are given in table 4. In this table we have also given the distances and coordination numbers obtained by curve fitting the data to equation (2). There is a good agreement between the distances and coordination numbers determined from Fourier transform and those obtained from curve-fitting. There is also a fair agreement between

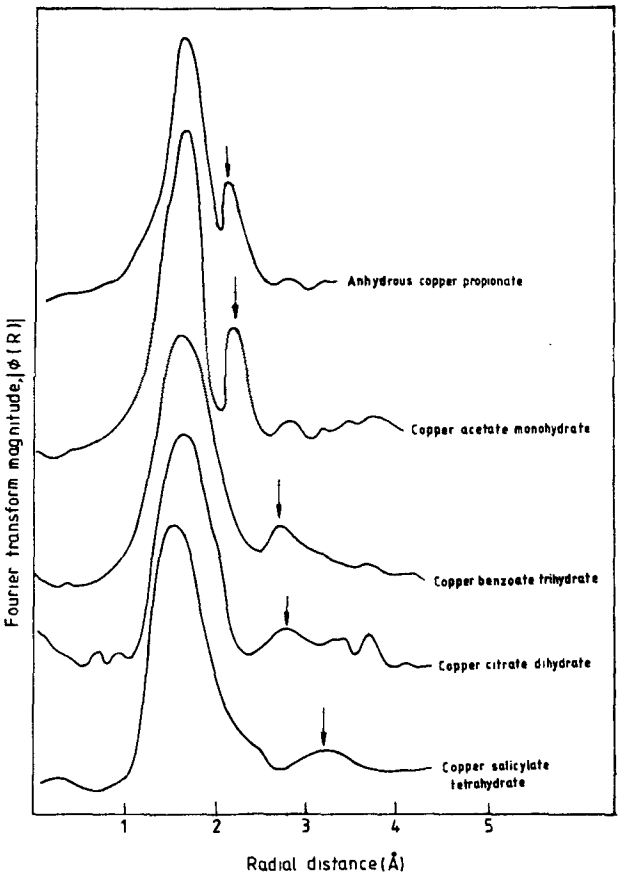

Figure 10. Fourier transforms of anhydrous copper propionate, copper acetate monohydrate, copper benzoate trihydrate, copper citrate dihydrate and copper salicylate tetrahydrate.

Table 4. Calculation of two-shell scatterer distances and numbers in copper carboxylates. Model compound: $Cu(CH_3CH_2COO)_2$.

Compound	Value of the fitting function	C_0	a_1	Radial distance		Coordination number	
				FT distance (Å)	Curve-fit distance (Å)	FT number	Curve-fit number
Copper acetate monohydrate							
(i) 4Cu–O at 1·969 Å	0·75	0·446	3·525	1·984	1·980	4·5	4·2
(ii) 1Cu–Cu at 2·614 Å		2·532	5·070	2·591	2·595	1·3	1·2
Copper benzoate trihydrate							
(i) 4Cu–O at 1·94 Å	0·98	0·418	3·447	1·950	1·934	4·3	4·1
(ii) 1Cu–Cu at 3·15 Å		0·980	6·198	3·180	3·160	0·8	0·9
Copper citrate dihydrate							
(i) 4Cu–O at 1·946 Å	0·81	0·403	3·456	1·951	1·947	3·9	3·9
(ii) 1Cu–Cu at 3·242 Å		0·967	6·390	3·250	3·240	0·7	0·8
Copper salicylate tetrahydrate							
(i) 4Cu–O at 1·92 Å	0·99	0·402	3·426	1·94	1·93	3·9	4·1
(ii) 1Cu–Cu at 3·728 Å		0·971	7·56	3·76	3·74	0·8	0·9

these data and the crystallographic data reported in literature.

Except for the acetate and the propionate where the Cu–Cu distance is less than 2·80 Å, there is no strong metal-metal peak in the Fourier transform of the benzoate or the citrate or the salicylate. Since the EXAFS amplitude is strongly dependent on the thermal motion of the backscatterers with respect to the absorbing atom, it is possible that at lower temperature metal-metal components can be more clearly distinguished in the FT spectra.

Acknowledgement

The authors thank the Department of Science and Technology, Government of India for support of this research and Prof. R J Magee for interesting them in the Cu complex formed by *Pseudomonas aeruginosa.*

References

Arjomand M and Machin D J 1975 *J. Chem. Soc. Dalton Trans.* 1061
Ashley C A and Doniach S 1975 *Phys. Rev.* **B11** 1279
Asbrink S and Norrby L J 1970 *Acta Crystallogr.* **B26** 8
Bacon G E and Curry N A 1962 *Proc. R. Soc. (London)* **A266** 95
Basu G, Belford R L and Dickerson R E 1962 *Inorg. Chem.* **1** 438
Belli M, Scafati A, Bianconi A, Mobilio S, Palladino L, Reale A and Burattini E 1980 *Solid State Commun.* **35** 355
Brauer G 1963 *Handbook of preparative inorganic chemistry* (New York: Academic Press)
Brown G M and Chidambaram R 1973 *Acta Crystallogr.* **B29** 2393
Citrin P H, Kincaid B M and Eisenberger P 1976 *Phys. Rev. Lett.* **36** 1346
Cramer S P and Hodgson K O 1979 *Prog. Inorg. Chem.* **25** 1
Cramer S P, Eccles T K, Kutzler F, Hodgson K O and Doniach S 1976 *J. Am. Chem. Soc.* **98** 8059
Cramer S P, Hodgson K O, Stiefel E I and Newton W E 1978 *J. Am. Chem. Soc.* **100** 2748
Grunes L A 1983 *Phys. Rev.* **B27** 2111
Harrison S E and Assour J M 1964 *J. Chem. Phys.* **40** 365
Himmelblau D M 1972 *Applied non-linear programming* (New York: McGraw-Hill)
Inoue M, Kishita M and Kubo M 1964 *Inorg. Chem.* **3** 239
Inoue M, Kishita M and Kubo M 1965 *Inorg. Chem* **4** 626
Lee P A, Teo B K and Simons A L 1977 *J. Am. Chem. Soc.* **99** 3856
Lytle F W, Sayers D E and Stern E A 1975 *Phys. Rev.* **B11** 4825
Magee R J 1981 Personal communication
Mastropaolo D, Powers D A, Potenza J A and Schugar H J 1976 *Inorg. Chem.* **15** 1444
Mazzi F 1955 *Acta Crystallogr.* **8** 137
Parthasarathy R, Sarode P R, Rao K J and Rao C N R 1982 *Proc. Indian Natl. Acad.* **A48** 119
Payne R, Magee R J, Sarode P R and Rao C N R 1981 *Inorg. Nucl. Chem. Lett.* **17** 125
Sankar G, Sarode P R and Rao C N R 1983 *Chem. Phys.* **76** 435
Shulman R G, Yaffet Y, Eisenberger P and Blumberg W E 1976 *Proc. Natl. Acad. Sci. USA* **73** 1384
Simonov Y A and Malinovskii T I 1970 *Sov. Phys. Cryst.* **15** 310.
Srivastava U C and Nigam H L 1972 *Curr. Sci.* **41** 81
Stern E 1974 *Phys. Rev.* **B10** 3207
Teo B K 1981 *in EXAFS spectroscopy: Techniques and applications* (eds) B K Teo and D C Joy, Chapter 3 (New York: Plenum)
Teo B K and Lee P A 1979 *J. Am. Chem. Soc.* **101** 2815
Via G H, Sinfelt J H and Lytle F W 1979 *J. Chem. Phys.* **71** 690